Industrial Health 2015, **53**, 78–84

Original Article

Characterization of ambient particles size in workplace of manufacturing physical fitness equipments

Chih-Chung LIN[2], Mei-Ru CHEN[3], Sheng-Lang CHANG[1], Wei-Heng LIAO[1] and Hsiu-Ling CHEN[1]*

[1]Institute of Occupational Safety and Hazard Prevention, Hung Kuang University, Taiwan
[2]Department of Environmental Science and Engineering, National Pingtung University of Science and Technology, Taiwan
[3]Department of Occupational Safety and Health, Chung Hwa University of Medical Technology, Taiwan

Received August 4, 2014 and accepted October 6, 2014
Published online in J-STAGE October 17, 2014

Abstract: The manufacturing of fitness equipment involves several processes, including the cutting and punching of iron tubes followed by welding. Welding operations produce hazardous gases and particulate matter, which can enter the alveolar, resulting in adverse health effects. This study sought to verify the particle size distribution and exposure concentrations of atmospheric air samples in various work areas of a fitness equipment manufacturing industry. Observed particle concentrations are presented by area and in terms of relative magnitude: painting (15.58 mg/m^3) > automatic welding (0.66 mg/m^3) > manual welding (0.53 mg/m^3) > punching (0.18 mg/m^3) > cutting (0.16 mg/m^3). The concentrations in each of the five work areas were $C_{inh}>C_{thor}>C_{resp}$. In all areas except the painting area, extra-fine particles produced by welding at high temperatures, and further those coagulated to form larger particles. This study observed bimodal distribution in the size of welding fume in the ranges of 0.7–1 μm and 15–21 μm. Meanwhile, the mass concentrations of particles with different sizes were not consistent across work areas. In the painting area, the mass concentration was higher in $C_{head}>C_{th}>C_{alv}$, but in welding areas, it was found that $C_{alv}>C_{head}>C_{th}$. Particles smaller than 1μm were primarily produced by welding.

Key words : Welding, Particle size, Inhalable, Respirable, Alveolar

Introduction

The manufacturing of fitness equipment includes cutting and punching iron tubes followed by welding and painting. Welding produces gaseous and particulate hazards containing metals[1–3], reactive oxygen species (ROS), and gases[4] from the base metal, welding electrode, and flux materials. A previous study identified three distinct types of welding fume particles ranging from 0.25 to 16 μm (aerodynamic diameter) in the breathing zone of welders[5]. Antonini[6] reported particles ranging from 0.50–2.0 μm. The diameters of fume particles produced by stainless-steel welding range from 0.02 μm to 0.81 μm (with an average of 0.1 μm and geometric standard deviation of 1.42)[7], and the mass-median aerodynamic diameter (MADD) of the particles in stainless-steel welding fumes was reported to be 0.255 μm[8]. Chung and Scott[9] reported that the aero-

*To whom correspondence should be addressed.
E-mail: hsiulin@sunrise.hk.edu.tw

dynamic equivalent diameter ranged from 0.26–0.56 μm in metal inert gas (MIG) and gas metal arc welding (GMAW); however, Moroni[10] observed larger particles, ranging from 0.44 to 6.16 μm in MIG welding fumes. Zimmer *et al.*[11] observed aerosols with diameter of 6.8 μm produced by GMAW. These studies have demonstrated that the particles in welding fumes range from ultrafine to fine. The fine particles produced in the high temperatures associated with welding are generally composed of spherical and aggregate particles[12]. Due to the high metal content and ROS within the welding environment[4, 13], preventing exposure is critical to the industrial health of workers. Three types of particles are produced during welding[14]: (1) particles (diameter >1 μm) dispersed by high temperature from the pool of metal liquid at the welding base during the melting process; (2) extra-fine particles (diameter <0.1 μm) /produced through evaporation, caused by a reaction between the welding base and electronic arc; (3) the collision of extra-fine particles causing the formation of particles with a diameter over 0.1–0.2 μm but less than 2–3 μm. Voitkevich *et al.*[15] identified the abundant Fe, Mn, Si, Ca, K, Na, and F in extra-fine particles, while those found in coarse particles were Fe and dissolved metals. The interactions of toxic metal components in fine and coarse particles of welding fumes have been discussed in previous studies[16]. The penetration mass of ultrafine titanium dioxide particles (aerodynamic diameter=20 nm) into the pulmonary interstitium is greater than that of fine particles (aerodynamic diameter=250 nm). The 12-wk pulmonary clearance of inhaled ultrafine particles is slower (t1/2=501 d) than that of larger particles (t1/2=174 d)[17]. This study sought to verify the particle size distribution and exposure concentration of atmospheric aerosols in the work areas of a fitness equipment manufacturing industry, in which the major fabrication procedure is welding. Due to the workers in this kind of industry wear the cotton-fabric mask, surgical mask or activated-carbon mask even they work in different areas where exist alternative exposure status. Therefore, it is expected that our results will provide a valuable resource for developing the environmental control strategies or making the right decision for the workers to use respiratory protective equipments to prevent particulate and gaseous hazards exposure.

Methods

Air sampling

Inhalable particles

Analysis was performed in a fitness equipment manufacturing industry in central Taiwan. The fabrication process is as follows: cutting steel tubes, punching holes in the steel tubes, welding steel tubes, painting the tubes, assembling the branched tubes, testing, and packing. Air samples were taken in each area associated with the six fabrication processes using an IOM personal inhalable aerosol sampler (SKC, Inc., Eighty-four, PA, USA, Institute of Occupation Medicine, IOM NO. 225-70A) with 25 mm diameter mixed cellulose ester filters (MCE, SKC) and set the flow rate at 2.0 l/min over a period of 7–8 h. The sampling time is August and September of 2012, and the temperature range from 31–35 °C and relative humidity range from 66–82%.

Particle size segregation

Air samples were obtained using an eight-stage cascade impactor (Personal Cascade MarpleImpactor Model 225-50-001; SKC Inc., Eighty Four, PA, USA) with 0.8 μm pores and 34 mm diameter mixed cellulose ester filters (MCE, SKC) and set the flow rate at 2.0 l/min over a period of 7–8 h. The sampling site is behind the worker about 1 meter. The particles ranged in size (aerodynamic diameter) as follows: <0.4 (back-up filter), 0.4–0.7, 0.7–1.0, 1.0–3.5, 3.5–6.5, 6.5–10, 10–15, 15–21, >21 μm and 50% cut-off aerodynamic ($d_{50\%}$) were 0.52, 0.96, 1.55, 3.5, 6.0, 9.8, 14.8, 21.3 μm. Mucilage was sprayed on the filters prior to sampling to prevent the particles from bouncing. The filters were maintained under the same conditions of temperature and humidity during pre- and post-sampling. The filters were weighed 48 h post-conditioning and post-sampling weights were subtracted from the pre-sampling weights to determine the mass of the particles obtained during ambient sampling. Personal air pump samplers with a flow rate of 2.0 l/min were used. IOM and Marple cascade impactor sampling heads were collected from the areas associated with punching, manual welding, automatic welding, painting, and cutting. All samples were obtained simultaneously and all results are the average of three samples. Thus, this study obtained a total of 15 size segregating samples.

Data analysis

Particle mass concentration

Due to the log-normality of each concentration, this study adopted the method of the minimum variance unbiased estimated (MVUE) for the estimation of the arithmetic mean (AM_{MVUE}), which was used to describe the average concentrations of all sizes particles. We then obtained the 95% CI to describe the log-normal distribution of particle size. This method of calculation was previously used by Chen *et al*. (2007)[18].

Particle size distribution for each process of fabrication

Particle size distribution was determined according to the average of three samples from each area associated with the five processes involved in fabrication. Particle size distribution was described according to mass median aerodynamic diameter (MMAD) and geometric standard deviation (GSD) estimated by $d_{50\%}$ and $d_{84\%}/d_{50\%}$, where $d_{n\%}$ represents the aerodynamic diameter at d_{ae} with an $n\%$ cumulative fraction for the given size distribution. $MMAD_c$, and GSD_c were reported as the coarse particles for $d_{ae} \geq 3.5$ μm and $MMAD_f$ and GSD_f were as fine mode (for $d_{ae} < 3.5$ μm).

Particle concentrations in various regions of the respiratory tract

The ratio of inhalable fraction, thoracic fraction, and respirable fraction was estimated using the data IOM and Marple cascade impactor sampling heads. This study adopted the inhalable, thoracic, and respirable sampling criteria outlined by the International Standards Organization (ISO), the Committee European de Normalisation (CEN), and ACGIH[19–21], as follows:

a. Inhalable particles: the fraction of particles aspirated through the nose or mouth during breathing.

b. Thoracic particles: the fraction of inhaled particles that passes into the lungs below the larynx.

c. Respirable aerosol: the fraction of inhaled particles that passes down to the alveolar, the gas exchange region of the lungs.

In the present study, the ratios of inhalable, thoracic, and respirable fractions were used to estimate the thoracic and respirable fractions of welding particles (C_{thor} and C_{resp} respectively) based on concentrations of inhalable particles (C_{inh}). The concentrations of welding particles in the head region ($C_{head}=C_{inh}-C_{thor}$), tracheobronchial region ($C_{th}=C_{thor}-C_{resp}$), and alveolar region ($C_{alv}=C_{res}$) were determined using personal air samplings in accordance with the definition of inhalable, thoracic, and respirable particles[18].

Results

Particle size distribution

Table 1 summarizes the concentrations (including AM_{MVUE} and 95% CI) of inhalable (C_{inh}), thoracic (C_{thor}) and respirable (C_{resp}) particles in each of the work areas. The particle concentrations in each area were as follows: painting (15.58 mg/m^3) > automatic welding (0.66 mg/m^3) > manual welding (0.53 mg/m^3) > punching (0.18 mg/m^3) > cutting (0.16 mg/m^3). With the exception of samples obtained from the painting area, all of the above concentrations were below the permissible exposure level (PEL) designated by the Taiwanese government (5 mg/m^3), as well as stands for Occupational Safety and Health Administration Permissible Exposure Level (OSHA PEL). The relative magnitude of the concentrations in each of the five work areas were as follows: $C_{inh}>C_{thor}>C_{resp}$, but the significant differences among C_{inh}, C_{thor}, C_{resp} were only observed in painting and manual welding areas.

Table 2 presents the MMAD and GSD for coarse mode (i.e., $MMAD_c$, GSD_c for $d_{ae} \geq 3.5$ μm) and fine mode (i.e., $MMAD_f$, GSD_f for $d_{ae} < 3.5$ μm), representing the size distributions of particles in this study. $MMAD_c$ values indicate that the particle size differed very little between work areas: cutting area (9.65 μm) and automatic welding area (9.93 μm). $MMAD_f$ values were as follows: painting (1.20 μm) > cutting (0.84 μm) > punching≈ automatic welding≈ manual welding (0.66–0.68 μm). Figure 1 presents the particle size distributions in each of the work

Table 1. Mean inhalable (C_{inh}), thoracic (C_{thor}), and respirable (C_{res}) concentrations and their 95% CI of the personal sampling in workers in different working processes (mg/m^3)

Areas	Painting	Manual welding	Automatic welding	Pouching	Cutting
n	3	6	6	3	3
Inhalable	15.58	0.53	0.66	0.18	0.16
Range	13.10–19.45	0.36–0.82	0.39–1.16	0.08–0.24	0.11–0.19
Thoracic	9.09	0.38	0.5	0.12	0.11
Range	8.02–10.36	0.25–0.58	0.29–0.97	0.06–0.16	0.08–0.13
Respirable	3.69	0.28	0.38	0.08	0.08
Range	3.43–3.92	0.17–0.41	0.22–0.79	0.04–0.11	0.06–0.09
p value	0.024*	0.023*	0.127	0.329	0.111

*: Significant differences were found among C_{inh}, C_{thor}, C_{resp} particles by Kruskal-Wallis test ($p<0.05$)

Table 2. Fine and coarse particle size distribution (MMAD) and geometric mean (GSD) of air samples at different working processes (mg/m^3)

Area	Fine particle			Coarse particle		
	$MMAD_f$	GSD_f	Fraction	$MMAD_c$	GSD_c	Fraction
	(µm)	(µm)	(%)	(µm)	(µm)	(%)
Painting (n=3)	1.2	2.76	19.1	9.71	1.78	80.9
Manual welding (n=6)	0.66	2.39	50.4	9.8	1.73	49.6
Automatic welding (n=6)	0.68	2.91	52.1	9.93	1.73	47.9
Punching (n=3)	0.68	2.04	44.4	9.74	1.69	55.6
Cutting (n=3)	0.84	2.84	47.3	9.65	1.82	52.7

Table 3. Estimated particle exposure concentrations and their 95% CI at the head (Chead), tracheobronchial (Cth) and alveolar (Calv) regions of the personal sampling in workers at different working processes (mg/m^3)

		Painting	Manual welding	Automatic welding	Punching	Cutting
	n	3	6	6	3	3
C_{head}	Mass conc.	6.49	0.14	0.17	0.06	0.05
	SD	5.07–9.09	0.1–0.24	0.1–0.21	0.02–0.11	0.03–0.06
	%	41.7	27.0	25.1	35.0	29.7
C_{th}	Mass conc.	5.4	0.1	0.11	0.04	0.03
	SD	4.59–6.65	0.07–0.17	0.07-0.18	0.02–0.04	0.02–0.04
	%	34.7	19.4	16.8	19.8	19.0
C_{alv}	Mass conc.	3.69	0.28	0.38	0.08	0.08
	SD	3.43–3.92	0.17–0.41	0.22–0.79	0.04–0.11	0.06–0.09
	%	23.7	53.6	58.1	45.1	51.3
	p value	0.051	0.003*	0.001*	0.300	0.052

*: Significant differences were found among C_{head}, C_{th}, Calv particles by Kruskal-Wallis test ($p<0.05$)

areas. Two modes of particle distribution were observed in the air samples obtained in the areas of manual welding, automatic welding, punching, and cutting. As shown in Fig. 2, the cumulative mass fraction of particles with alternative particle size exhibited a obviously accumulation of mass concentration was found in large particle size in the painting area, that differed from other working areas.

Estimation of particle concentration in various regions of the respiratory tract

Table 3 presents the particle concentrations in the head region (C_{head}), tracheobronchial region (C_{th}), and alveolar region (C_{alv}) of the respiratory tract. Once again, we see a similar pattern in the relative magnitudes of the concentrations: painting>automatic welding>manual welding>punching>cutting. Significant differences were observed among C_{head}, C_{th}, C_{alv} in the painting, manual welding, and automatic welding areas. However, the mass concentrations of different size intervals were not consistent among each of the work areas. In the painting area, the mass concentration was as follows: $C_{head}>C_{th}>C_{alv}$. In the welding areas, the mass concentration was as follows: $C_{alv}>C_{head}>C_{th}$. The highest levels were obtained for C_{alv} in the welding, cutting, and punching areas.

Discussion

Particle concentrations of welding fume

Flynn *et al.*[22] reported average inhalable particle concentrations of 4.72 mg/m^3 (0.003–60 mg/m^3) in welders according to data provided by Occupational Safety and Health Administration (OSHA) in 1978–2008. Those values were higher than the data obtained in the present study (0.53–0.66 mg/m^3). Variations in welding fume concentration may be due to the environment in which welding was performed (indoors vs. outdoors) as well as ventilation conditions. Lehnert *et al.*[23] reported the median level of respirable particles as 0.21 mg/m^3 for tungsten inert gas

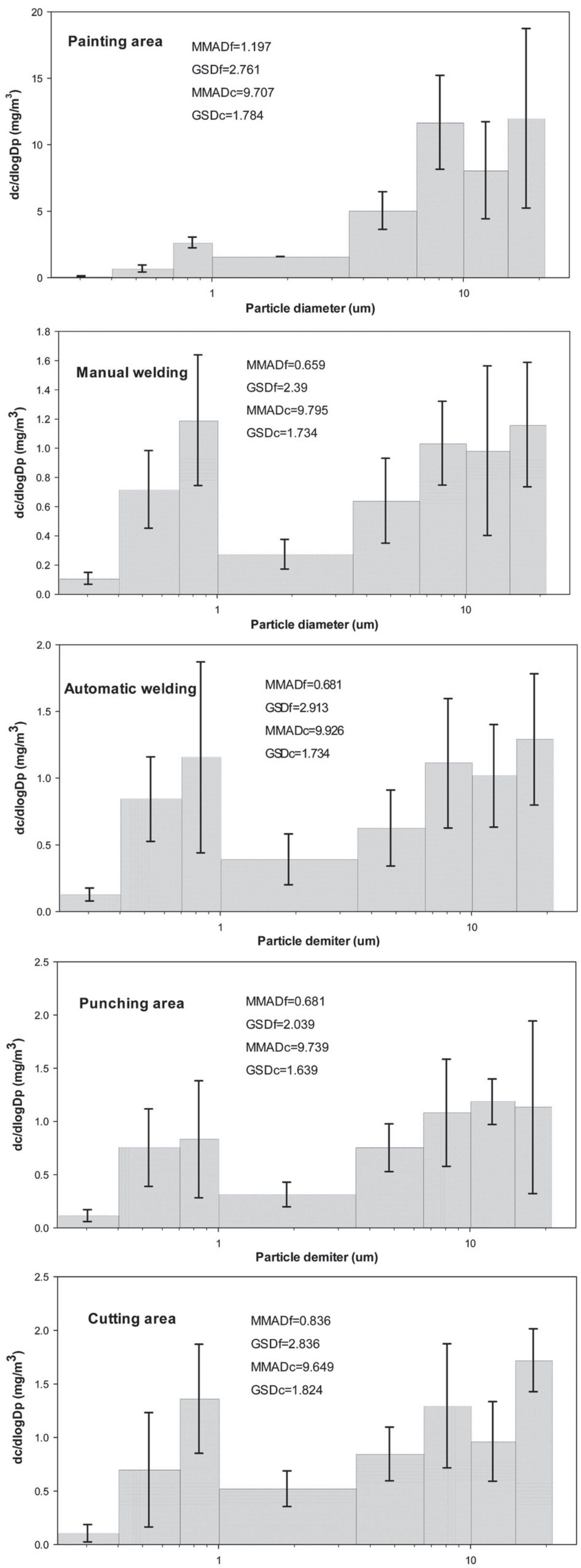

Fig. 1. Particle size distribution of ambient particle collected from workplaces of welding, pouching, cutting and painting process in the fitness equipments manufacturing industry.

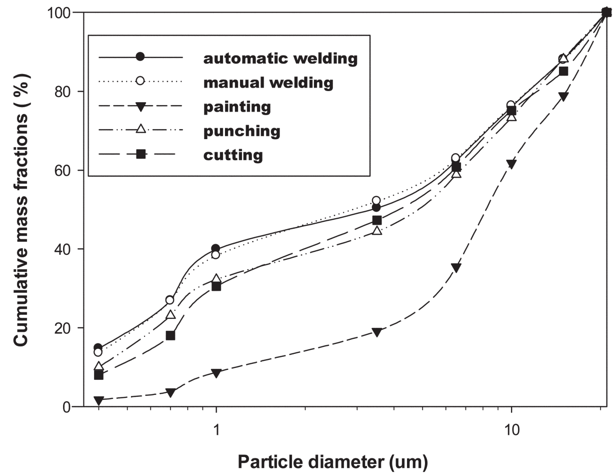

Fig. 2. Cumulative mass fraction of particles with alternative particle size in workplaces of welding, pouching, cutting and painting process in the fitness equipments manufacturing industry.

(TIG) welding and 1 mg/m^3 for gas metal arc welding (GMAW), which are in strong agreement with the data obtained in the current study (0.28–0.38 mg/m^3). In different working areas, due to the significant differences of C_{inh}, C_{thor}, C_{resp} were only observed in painting and manual welding areas, it is inefficient for the workers who wore the cotton fabric mask and surgical mask in preventing occupational exposure with wide range concentration in different particle size of the two areas in the prevent study. Yu *et al.*[7)] reported that welding particulates with the mean particle diameter of 0.1 μm deposited in the lower respiratory tract, including bronchioles, alveolar ducts, alveolar sacs, and alveoli. Though the present result indicated that the particle size of welding particulates was <1 μm, the particle-size distribution, morphology and chemical aspects of the resultant fumes may be affected by the welding alloy[11)], and the particle size may change dynamically with time[24)].

Particle concentrations in various regions of the respiratory tract

In the painting area, higher particle concentrations were obtained in the head region (41.7%). The highest particle concentrations in the alveolar region were obtained in the manual welding (53.6%) and automatic welding areas (58.3%). These results indicate that fine particles produced during welding enter the tracheobronchial and alveolar regions, especially for very fine particles, which can enter alveolar regions and cannot be exhaled through expiratory flow[25)]. Although in the point of particles size, for similar mass concentrations, welding fumes are considered more harmful than the particles generated in the painting area, the hazardous effect should considered the chemical composition in alternative aerosols, those in the welding fume are different from that of the painting aerosol. Therefore, the particle size and chemical composition should be further analyzed simultaneously in comprehensive consideration in this kind of working characteristics.

Though the MMAD of coarse particles were nearly equal in the painting, cutting, punching, and welding areas, for MMAD of fine particles, those were less than 1 μm in cutting, punching, and welding areas (0.66–0.68 μm) except for painting area. These results match those of Jenkins and Zimmer *et al*.[24, 26] James *et al.*[27] reported that the MMAD of high-solids basecoat paint overspray aerosols ranged from 2.9 to 9.7 μm; this result is equal to the particle size distribution found in this study. Sowards *et al.*[14] classified fume particles according to three distinct morphologies: spherical, irregular, and agglomerate. They observed bimodal distribution among inorganic aerosols, such as aluminum or steel; however, organic compounds presented a single or poly-dispersed mode in the size-fractionated particulate samples, with MMAD similar to that of total overspray aerosol[27]. In Fig. 2, the highest concentration was obtained for particles in the range of 0.7–1.0 μm, followed by 15–21 μm, illustrating bimodal distribution. The aggregate modal may help to solve the dynamics of particles involved in generation, convection, diffusion, coagulation, and coalescence in a spatially two-dimensional flame system[28]. Spatial transport processes may influence aerosol dynamics, and thermophores have the greatest impact on the spatial distribution of aerosol mass[29]. The two main modals of the particle size in the range of 0.7–1 μm and 15–21 μm both existed in automatic welding and manual welding areas.[30, 31] determined that the size and morphology of particles are strongly affected by flame temperature and transport processes within the flame. This may explain the formation of extra-fine particles produced during high-temperature welding, followed by the coagulation of these particles to form larger particles. In the punching and cutting areas, coarse particles were found to be of the highest concentration (>3.5 μm). In particular, the cutting areas exhibited a highest level in 15–21 μm of coarse particles. Thornburg and Leith[32] reported that a metal shearing machine with lower viscosity could result in the generation of large MMAD (21.9 μm) of oil droplets. In terms of extra-fine particles, the cutting fluid applied in the cutting or punching process results in a greater impaction force, which might lead to the generation of oil droplets of a lower MMAD[18, 32]. These small droplets may be produced by two mechanisms: atomization and vaporization condensation[33]. In Fig. 2, the distribution of particles in the automatic and manual welding process was coherent with three slopes. These trends could be interpreted as follows: (1) <1μm particles might be produced from high-temperature flames; (2) 1–6.5 μm particles might be the result of extra-fine particles coagulating; (3) 6.5–21 μm particles may be formed by machine force in the cutting and punching areas[25].

Conclusion

The mass concentration of welding fumes is higher than those without operating welding work. This study observed bimodal distribution in the size of welding particles in the ranges of 0.7–1 μm and 15–21 μm. The most predominant concentration is in alveolar region due to the most aerodynamic diameter of the welding particles are below than 1 μm.

Acknowledgement

This study was financially supported by grants from the Council of Labor Affairs in Taiwan grants.

References

1) Antonini JM, O'Callaghan JP, Miller DB (2006) Development of an animal model to study the potential neurotoxic effects associated with welding fume inhalation. Neurotoxicology **27**, 745–51.
2) McNeilly JD, Heal MR, Beverland IJ, Howe A, Gibson MD, Hibbs LR, MacNee W, Donaldson K (2004) Soluble transition metals cause the pro-inflammatory effects of welding fumes in vitro. Toxicol Appl Pharmacol **196**, 95–107.
3) McNeilly JD, Jiménez LA, Clay MF, MacNee W, Howe A, Heal MR, Beverland IJ, Donaldson K (2005) Soluble transition metals in welding fumes cause inflammation via activation of NF-kappaB and AP-1. Toxicol Lett **158**, 152–7.
4) Liu HH, Wu YC, Chen HL (2007) Production of ozone and reactive oxygen species after welding. Arch Environ Contam Toxicol **53**, 513–8.
5) Oprya M, Kiro S, Worobiec A, Horemans B, Darchuk L, Novakovic V, Ennan A, Van Grieken R (2012) Size distribution and chemical properties of welding fumes of inhalable particles. J Aerosol Sci **45**, 50–7.
6) Antonini JM (2003) Health effects of welding. Crit Rev Toxicol **33**, 61–103.

7) Yu IJ, Kim KJ, Chang HK, Song KS, Han KT, Han JH, Maeng SH, Chung YH, Park SH, Chung KH, Han JS, Chung HK (2000) Pattern of deposition of stainless steel welding fume particles inhaled into the respiratory systems of Sprague-Dawley rats exposed to a novel welding fume generating system. Toxicol Lett **116**, 103–11.
8) Antonini JM, Stone S, Roberts JR, Chen B, Schwegler-Berry D, Afshari AA, Frazer DG (2007) Effect of short-term stainless steel welding fume inhalation exposure on lung inflammation, injury, and defense responses in rats. Toxicol Appl Pharmacol **223**, 234–45.
9) Chung KYK, Scott RM (1997) Particle-size analysis of welding fume. J Aerosol Sci **28**, 339.
10) Moroni B, Viti C (2009) Grain size, chemistry, and structure of fine and ultrafine particles in stainless steel welding fumes. J Aerosol Sci **40**, 938–49.
11) Zimmer AT, Baron PA, Biswas P (2002) The influence of operating parameters on number-weighted aerosol size distribution generated from a gas metal arc welding process. J Aerosol Sci **33**, 519–31.
12) Chang JS, Looy PC, Brocilo D, Berezin AA, Duffy WD, Schaap D, Moeller KR (2000) Characterization of particles generated by thermal plasma welding of galvanized steels. J Aerosol Sci **31**, 672–3.
13) Cohen MD, Zelikoff JT, Chen LC, Schlesinger RB (1998) Immunotoxicologic effects of inhaled chromium: role of particle solubility and co-exposure to ozone. Toxicol Appl Pharmacol **152**, 30–40.
14) Sowards J, Ramirez A, Dickinson D, Lippold J (2010) Characterization of Welding Fume from SMAW Electrodes? Part II. Weld Res **89**, 82s–90s.
15) Voitkevich VG (1982) Methods for studying welding fumes The Paton. Weld J **3**, 51–4.
16) Worobiec A, Stefaniak E, Kiro S, Oprya M, Bekshaev A, Spolnik Z, Potgieter VS, Ennan A, Van Grieken R (2007) Comprehensive micro analytical study of welding aerosols with X-Ray and Raman based methods. XRay Spectrom **36**, 328–35.
17) Ferin J, Oberdörster G, Penney DP (1992) Pulmonary retention of ultrafine and fine particles in rats. Am J Respir Cell Mol Biol **6**, 535–42.
18) Chen MR, Tsai PJ, Chang CC, Shih TS, Lee WJ, Liao PC (2007) Particle size distributions of oil mists in workplace atmospheres and their exposure concentrations to workers in a fastener manufacturing industry. J Hazard Mater **146**, 393–8.
19) Comitéeuropéen de normalization (CEN) (1992), Workplace atmosphere: size fraction definitions for measurement of airborne particles in the workplace, CEN, Brussels (Standard EN 481).
20) International Standard Organization (ISO) (1992), Air quality-particle size fraction definitions for health-related sampling, International Standards Organization, Geneva (ISO CD7708).
21) American Conference of Governmental Industrial Hygienists (ACGIH) (1993–1994), Threshold limit values for chemical substances and physical agents and biological exposure indices, ACGIH, Cincinnati, 42–45.
22) Flynn MR, Susi P (2010) Manganese, iron, and total particulate exposures to welders. J Occup Environ Hyg **7**, 115–26.
23) Lehnert M, Pesch B, Lotz A, Pelzer J, Kendzia B, Gawrych K, Heinze E, Van Gelder R, Punkenburg E, Weiss T, Mattenklott M, Hahn JU, Möhlmann C, Berges M, Hartwig A Brüning T, Weldox Study Group (2012) Exposure to inhalable, respirable, and ultrafine particles in welding fume. Ann Occup Hyg **56**, 557–67.
24) Zimmer AT, Biswas P (2001) Characterization of the aerosols resulting from arc welding processes. J Aerosol Sci **32**, 993–1008.
25) Konarski P, Iwanejko I, Cwil M (2003) Core-shell morphology of welding fume micro-and nanoparticles. Vacuum **70**, 385–9.
26) Jenkins NT, Pierce WMG, Eagar TW (2005) Particle size distribution of gas metal and flux cored arc welding fumes. Weld J **84**, 156s–63s.
27) D'Arcy JB, Chan TL (1990) Chemical distribution in high-solids paint overspray aerosols. Am Ind Hyg Assoc J **51**, 132–8.
28) Kim H, Jeong J, Park Y, Yoon Y, Choi M (2003) Modeling of generation and growth of non-spherical nanoparticles in a co-flow flame. J Nanopart Res **5**, 237–46.
29) Yu S, Yoon Y, Muller-Roosen M, Kennedy IM (1998) A two-dimensional discrete-sectional model for metal aerosol dynamics in a flame. Aerosol SciTechnol **28**, 185–96.
30) Lee D, Choi M (2002) Coalescence enhanced synthesis of nanoparticles to control size, morphology and crystalline phase at high concentrations. J Aerosol Sci **33**, 1–16.
31) Lee D, Yang SS, Choi M (2001) Controlled formation of mamoparticles utilizing laser irradiation in a flame and their characteristics. Appl Phys Lett **79**, 2459–61.
32) Thornburg J, Leith D (2000) Mist generation during metal machining. J Tribol **122**, 544–9.
33) Michalek DJ, Hii WWS, Sun J, Gunter KL, Sutherland JW (2003) Experimental and analytical efforts to characterize cutting fluid mist formation and behavior in machining. Appl Occup Environ Hyg **18**, 842–54.